Carbon-climate feedback higher when assuming Michaelis-Menten kinetics of respiration

Christian Beer[1, 2]

[1]Department of Earth System Sciences, University of Hamburg, Hamburg, 20134, Germany
[2]Center for Earth System Research and Sustainability, University of Hamburg, Hamburg, 20134, Germany

Correspondence to: Christian Beer (christian.beer@uni-hamburg.de)

Abstract.

Earth system models simplify complex terrestrial respiration processes assuming a first-order chemical reaction or assuming a Michaelis-Menten kinetics. The effect of the respective mathematical representation on the terrestrial carbon-climate feedback is unclear. Using a simplified model of biogeochemical feedbacks to climate, I show that the terrestrial carbon-climate feedback roughly doubles. Hence, the remaining carbon budget to keep global warming below 2 °C is 66-113 Pg C higher, when assuming Michaelis-Menten kinetics instead of first-order kinetics of respiration, but these differences depend on the underlying emission scenario. These results highlight the importance of an increased understanding of the respiration processes on a global scale for more reliably project future carbon dynamics and climate, related feedback mechanisms, and thus to estimate a valid remaining anthropogenic carbon budget using Earth System Models.

1 Introduction

The anthropogenic emission of carbon dioxide into the atmosphere since the industrialization period led to a global warming of about 1 K due to the greenhouse effect (Canadell et al., 2023). However, less than half of the anthropogenically emitted carbon remains in the atmosphere because terrestrial ecosystems and the ocean take up 34% and 25%, respectively (Friedlingstein et al., 2023). The main reasons for this strong carbon dioxide uptake in terrestrial ecosystems are biogeochemical feedbacks (Cox, Betts, Jones, Spall, & Totterdell, 2000). Increasing atmospheric carbon dioxide (CO_2) concentration leads to an enhanced photosynthesis rate, and hence to a CO_2 uptake by vegetation on land (Cramer et al., 2001; O'Sullivan et al., 2022). This carbon is stored in vegetation pools and ultimately transferred to soils by exudation, litterfall, and mortality processes, thereby increasing the soil carbon content. This is the important carbon-concentration feedback mechanism (Arneth et al., 2010) (Fig. 1) which is a negative feedback, hence responsible for the current net CO_2 sink on land that has been preventing us from an even stronger climate change. In contrast, autotrophic and heterotrophic respiration are also higher than under pre-industrial conditions (Canadell et al., 2023) due to i) higher substrate availability and ii) the positive temperature sensitivity of respiration (Lloyd & Taylor, 1994). This temperature sensitivity of respiration forms the positive carbon-climate feedback mechanism (Fig. 1): Higher CO_2 concentration leads to higher temperature, which increases respiration and hence leads to an even higher atmospheric CO_2 concentration (Arneth et al., 2010).

34
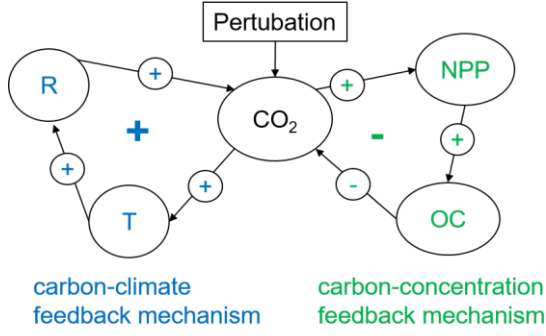
35 **Figure 1: Feedback diagram for two main terrestrial biogeochemical feedback mechanisms. NPP: Net primary**
36 **production, R: respiration, OC: land organic carbon stocks, T: global surface air temperature, CO_2: atmospheric**
37 **carbon dioxide content.**

38

39 These two biogeochemical feedback mechanisms have been identified as two major feedback mechanisms in the

40 Earth system with great impact on climate (Arora et al., 2020; Friedlingstein et al., 2006). Currently, the positive

41 carbon-climate feedback is lower than the negative carbon-concentration feedback and therefore land ecosystems

42 act as a natural sink of CO_2 of about 3 Pg C per year (Friedlingstein et al., 2023). However, due to internal dynamics

43 of the system, climate change, and changes in anthropogenic CO_2 emissions, the future strength of the feedback

44 mechanisms and hence the net CO_2 exchange between land and atmosphere remains unclear. Recent accumulation

45 of soil carbon in concert with higher future temperature and a declining increase in productivity can lead to a

46 decreasing land sink under increasing CO_2 emissions in future (Cramer et al., 2001; C. D. Jones et al., 2023). To

47 estimate such feedbacks, we need to run a modified version of an Earth System Model in which only one feedback

48 mechanism is considered. The temporal difference in atmospheric CO_2 concentration from such experiments to

49 model runs without the feedback is used to quantify these feedbacks (Hansen et al., 1984).

50 For the carbon-climate feedback mechanism (Fig. 1), the representation of respiration processes in Earth System

51 Models is crucial. Several assumptions about the underlying processes and respective mathematical

52 representations have been proposed. Land surface models usually represent respiration as a linear function (first-

53 order kinetics) to the amount of available substrate (organic carbon, C),

54 $\frac{dC}{dt} = -\mathrm{k} \cdot \mathrm{C}$ (1)

55 using several carbon pools (Brovkin et al., 2013; Sitch et al., 2003; Tang, Riley, & Zhu, 2022), with different

56 decomposition rate constants k. However, the underlying biochemical reactions are mostly enzymatic, hence a

57 Michaelis-Menten kinetics model should be more valid to represent the dynamics of respiration (Wieder, Bonan,

58 & Allison, 2013; Yu, Ahrens, Wutzler, Schrumpf, & Zaehle, 2020)

59 $\frac{dC}{dt} = v_{max} \frac{C}{K_M + C}$ (2)

60 where v_{max} is the maximum reaction rate under infinite carbon substrate C, and K_M represents the amount of

61 carbon at which the reaction rate is half of the maximum. The nonlinear shape of this relationship between reaction

62 rate and substrate availability (in contrast to the linear dependency of first-order kinetics models) leads to a steep

63 increase of the reaction rate under low substrate availability while only a moderate to negligible increase under

64 high substrate availability. In doing so, this model implicitly represents the function of enzymes in the underlying

65 biochemical reactions. Such model enables a more valid aggregation from the process level (e.g. rhizosphere,

66 aggregatusphere) to the landscape scale (Reichstein & Beer, 2008).

67   The two approaches represented by equations 1 and 2 imply different responses of respiration to changing substrate

68   availability. Therefore, future dynamics of respiration should differ depending on the mathematical formulation.

69   Such structural model uncertainty is in particular of interest because there might be a point when the land sink

70   starts to decrease even under continuing high anthropogenic emissions(Cramer et al., 2001), or for the question on

71   how land sinks will react to decreasing or even negative anthropogenic carbon emissions.

72   Therefore, I ask three main questions in this paper: What is the effect of the respiration model structure on

73   • projections of the land carbon sink

74   • the strength of the carbon-climate feedback

75   • the remaining anthropogenic carbon budget

76   under different carbon emission scenarios? To address these questions I performed a feedback analysis using a

77   simplified but process-based model of global biogeochemical feedback mechanisms twice, using a first-order and

78   a Michaelis-Menten kinetics model of respiration.

79   **2 Methods**

80   **2.1 Simplified Carbon-Climate Feedback Model**

81   The model has been designed to study the two major biogeochemical feedbacks to climate displayed in Fig. 1.

82   Exchanges of carbon among atmosphere, ocean and land are represented using a reduced number of carbon pools

83   without spatial details but still in a process-based way, i.e. based on a set of differential equations. For example,

84   the amount of carbon taken up by vegetation depends on the atmospheric carbon content while the amount of CO_2

85   released to the atmosphere due to respiration depends on the carbon content of the ecosystem. The model assumes

86   a global surface air temperature response to changing atmospheric carbon dioxide content using a transient climate

87   response parameter, which is lagged due to the ocean heat capacity. The model is driven by anthropogenic carbon

88   dioxide emissions to the atmosphere following several scenarios developed for the IPCC 6th assessment report.

89   A detailed description of the model can be found in (Lade et al., 2018). Here, I apply two alternative model

90   versions, one assuming a first-order kinetics of respiration (FOK), and one assuming a Michaelis-Menten kinetics

91   of respiration (MMK). The representation of terrestrial carbon uptake by gross primary productivity is identical in

92   both model versions. It is assumed to increase logarithmically with atmospheric carbon dioxide C_a (Equations 3

93   and 4, first term right-hand side). In addition, emissions due to land use change E_L are subtracted the same way in

94   both versions, and the increase in respiration with temperature is represented by a typical Q_{10} model (Equations 3

95   and 4, second term right-hand side). Only the dependence of respiration to land carbon stocks differs. The FOK

96   model assumes a first-order kinetics with a respiration rate constant estimated by pre-industrial GPP and carbon

97   stocks, $k = \frac{GPP_0}{C_{L,0}}$ following the same principle as in (Lade et al., 2018).

98    $$\frac{dC_L}{dt} = GPP_0 \left(1 + \alpha \log \frac{C_a}{C_{a,0}}\right) - Q^{\frac{\Delta T}{10}} \cdot k \cdot C_L - E_L \qquad (3)$$

99   In contrast, the MMK model represents respiration as a classical Michaelis-Menten equation with parameters v_{max}

100   and K_M:

101   $$\frac{dC_L}{dt} = GPP_0 \left(1 + \alpha \log \frac{C_a}{C_{a,0}}\right) - Q^{\frac{\Delta T}{10}} \cdot v_{max} \frac{C_L}{K_M + C_L} - E_L \qquad (4)$$

Parameters and pre-industrial pools and fluxes for model initialization were taken from (Lade et al., 2018) and partly adjusted (Table 1). The transient climate response to CO_2 doubling λ is set at the higher end of the range reported for CMIP6 model results (Arora et al., 2020; Nijsse, Cox, & Williamson, 2020) in order to match the observed historical temperature anomaly. Parameters v_{max} and K_M of Equation 4 are optimized using a standard gradient decent approach (MATLAB R 2023b function lsqnonlin) such that the difference of the modelled and observation-based land carbon changes is minimized.

Table 1. Value and description of parameters different from (Lade et al., 2018).

Name	Symbol	Value	Reference/comment
Pre-industrial soil and vegetation Carbon	$C_{L,0}$	2305 Pg C	Sum of vegetation and soils carbon stocks following (Canadell et al., 2023), and C stocks of the active layer of gelisols following (Hugelius et al., 2014)
Transient climate response to CO_2 doubling (TCR)	λ (Equation 10 of (Lade et al., 2018))	2.5 K	Tuning parameter, higher end of range of CMIP6 models (Arora et al., 2020; Nijsse et al., 2020)
Respiration sensitivity parameter	Q	2	(Vaughn & Torn, 2019)
Pre-industrial GPP	GPP_0	113 Pg C a^{-1}	(Friedlingstein et al., 2023)
CO_2 sensitivity of GPP	α	0.35	Tuning parameter (Alexandrov, Oikawa, & Yamagata, 2003)
Max respiration rate in MMK model	v_{max}	200 Pg C a^{-1}	Tuning parameter
Substrate concentration at half of max respiration rate in MMK model	K_M	1787 Pg C	Tuning parameter

2.2 Modeling protocol

The two model versions have been run from 1850 until 2100 using a daily time step forced by anthropogenic carbon dioxide emissions from fossil fuel burning and from land-use change. For this, I combined reported historical emissions from the Global Carbon Project (Friedlingstein et al., 2023) with Shared Socioeconomic Pathways (SSP) emission scenarios from the public database of the Institute for Applied Systems Analysis (Riahi et al., 2017). I selected four widely used scenarios produced for the CMIP6 protocol (Gidden et al., 2019): SSP1-26 (optimistic scenario, reaching economic growth while retaining sustainability and reducing inequalities), SSP2-45 (including mitigation strategies), SSP3-70 (represents a future of inequality and fossil fuel dependency), and

118   SSP5-85 (representing economic growth through strong reliance on fossil fuels). These scenarios reach a forcing

119   of 2.6, 4.5, 7.0, and 8.5 W/m² at the end of the century and represent a huge spread of carbon emissions into the

120   atmosphere (Fig. 2). I interpolated linearly the reported emissions at decadal scale to an annual resolution. In the

121   combined time series (Fig. 2), historical emissions span the period 1850-2014 and scenarios continue from 2015

122   until 2100.

123
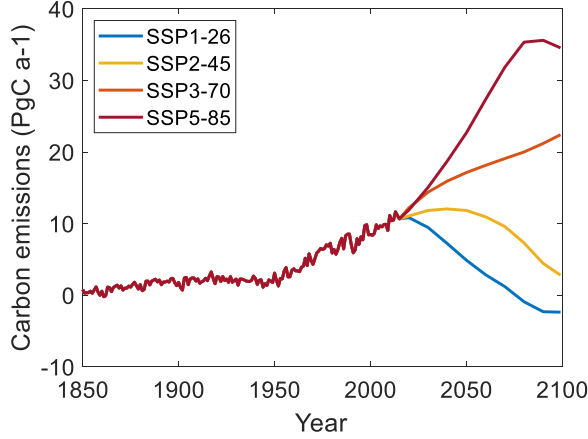
125   **Figure 2: Total CO₂ emissions from burning fossil fuels and land-use change from combining a historical dataset with**
126   **results from Integrated Assessment Models for different scenarios.**

127

128   I performed model simulations for these emission scenarios and for both model versions, FOK and MMK. The

129   results were used to evaluate the model during the historical period, and to estimate the remaining carbon budgets

130   to keep warming below a certain threshold. For the feedback analysis, all these simulations were repeated three

131   times. To estimate the feedback factor, I did model simulations in which only the terrestrial carbon-climate

132   feedback is considered. The results were used to estimate the respective ΔC_A^{on} (section 2.4). For calculating the

133   feedback sensitivities β and γ (Section 2.4), I additionally performed biogeochemically and radiatively coupled

134   simulations following (Friedlingstein et al., 2006; Lade et al., 2018) and derived ΔC_L, ΔC_A and ΔT from these

135   simulations. In the biogeochemically coupled simulation, I set λ to 0, hence effects of CO_2 change on temperature

136   are excluded. In the radiatively coupled simulation, I neglected all effects of CO_2 on terrestrial or marine carbon

137   pools. In total, that are 32 model simulations.

138

139   **2.4 Feedback analysis**

140   Atmospheric carbon content increases in time due to annual anthropogenic emissions (e_i) and internal feedback

141   mechanisms. To estimate this carbon dioxide change when considering a terrestrial carbon-climate feedback

142   ("on"), I averaged the atmospheric carbon content during a reference period in the future (2080-2100) and in the

143   past (1850-1900) using the respective model simulation (section 2.3), and subtract both:

144   $\Delta C_A^{on} = C_A^{future} - C_A^{past}$ (5).

145   The respective atmospheric carbon change without considering the feedback ("off") equals the sum of emissions:

146   $\Delta C_A^{off} = \sum_{i=1850}^{2100} e_i$ (6).

147 The feedback is the difference $\Delta C_A^{on} - \Delta C_A^{off}$ and the feedback factor F is the ratio of both changes, which can be

148 used to compare feedbacks and to identify positive (F>1) or negative feedbacks (F<1) (Cox et al., 2000;

149 Friedlingstein, Dufresne, Cox, & Rayner, 2003; Hansen et al., 1984; Zickfeld, Eby, Matthews, Schmittner, &

150 Weaver, 2011)

151 $F = \frac{\Delta C_A^{on}}{\Delta C_A^{off}}$ (7).

152 Sensitivities of the land carbon change to atmospheric carbon concentration (β) and temperature changes (γ) are

153 defined following (Friedlingstein et al., 2006; Heinze et al., 2019) as

154 $\Delta C_L = \beta \cdot \Delta C_A + \gamma \cdot \Delta T$ (8).

155 I used the biogeochemically coupled simulation results to estimate β (ΔT=0), and the radiatively coupled results

156 to estimate γ (ΔC$_A$=0).

157 **3 Results**

158 Model results of carbon fluxes and the surface temperature anomaly for the historical period are in general

159 agreement with results by the Global Carbon Project (Friedlingstein et al., 2023) and the NOAA Global Surface

160 Temperature record (Fig. 3), i.e. the overall historical trends are captured. The model does not represent spatial

161 details, oversimplifies functional diversity and does not represent certain processes, such as disturbances.

162 Therefore, the model is not able to capture the inter-annual variability of land carbon fluxes (Fig. 3). The general

163 long-term agreement shows that major biogeochemical feedback mechanisms are correctly represented, and that

164 initial conditions (Table 1) and model parameters (Table 1) are reasonable. Therefore, we assume that we can

165 apply this model to study the effects of structural respiration model uncertainty on the carbon-climate feedback

166 strength.

167

168
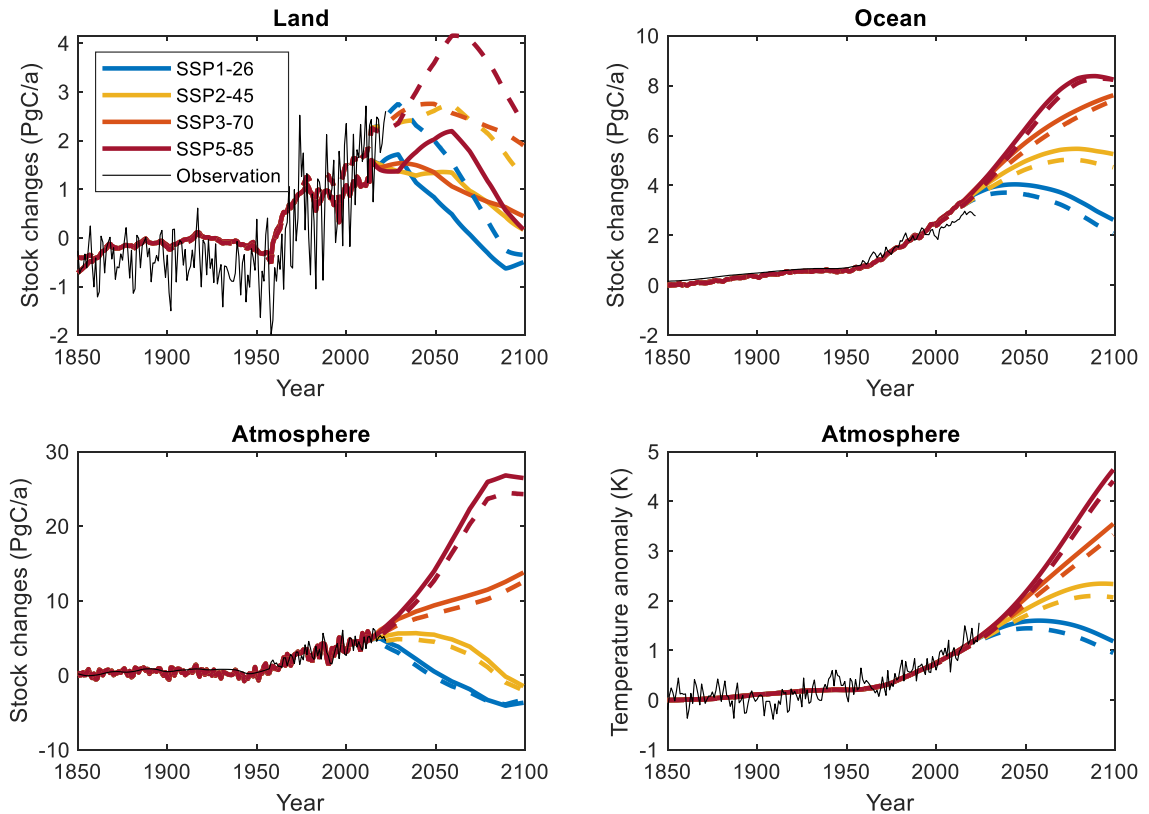
Figure 3: Simulated carbon fluxes and temperature anomaly for the different scenarios. FOK and MMK model results are displayed by solid and dashed lines, respectively. Simulation results are compared to estimates by the Global Carbon Project or to the NOAA Global Surface Temperature record, which has been bias corrected to the model results to match reference periods.

173

Figure 3 also shows the projections of carbon fluxes to land, ocean and atmosphere, as well as the temperature change for the two different model structures until 2100 following the different emission scenarios. Overall, these projections of the main carbon cycle fluxes and temperature change are similar to concentration-driven CMIP6 results (Canadell et al., 2023; Chris D. Jones et al., 2023). The projected ocean carbon sink in this study is substantially higher for most of the scenarios, and the land carbon sink of the model using a first-order kinetics respiration approach (FOK) is lower, but comparable with Lade et al. (2018). Otherwise, the projections of the change in atmospheric carbon stocks and the global surface temperature change are similar to studies using Earth System Models (Canadell et al., 2023). However, spread of carbon cycle projections using other models is usually also very high (Canadell et al., 2023; Chris D. Jones et al., 2023), and the uncertainty due to parameter values or initial conditions hardly quantified in these studies.

The projected land sink evolution differs depending on both, the emission scenario and the model structure applied. Under high emission scenarios, the land sink continues to rise and peaks in the middle of the century followed by a decreasing sink until 2100. This peak has been reported by DGVMs and ESMs before (Cramer et al., 2001; C. D. Jones et al., 2023) and is due to the reverse shape of the two main response functions, logarithmic productivity response to elevated CO_2 and quasi-exponential respiration response to temperature. A second reason is internal carbon dynamics: Respiration depends on the amount of land carbon stocks, which continued to increase until some maximum and therefore is the basis for a high respiration flux during the following time. For the scenario

SSP1-26, the land sink starts to decrease immediately after the historical period, i.e. when emissions are reduced, and depending on the model structure is getting even negative at the second half of the century.

The projected land carbon sink in 2100 is much higher when assuming a Michaelis-Menten kinetics model for respiration (MMK) even under an equal temperature sensitivity of respiration as by the first-order kinetics model (FOK), and even when parameters are chosen to fit both model results during the historical period. In addition, the peak in the middle of the century is more pronounced when using the MMK model (Fig. 3). Hence, this difference is only due to internal carbon dynamics differences, in particular a non-linear (decreasing) change of the respiration rate with increasing substrate availability under when assuming Michaelis-Menten kinetics. This clearly demonstrates the uncertainty of land carbon sink dynamics just due to alternative assumptions and mathematical formulations of respiration processes. As a result of higher land sinks using the MMK model, ocean and atmosphere sinks are smaller and the temperature change is lower (Fig. 3). Due to the higher land C sink assuming Michaelis-Menten kinetics, also total changes in land carbon stocks are much higher, i.e. land takes up several hundred of Pg C more depending on the emission scenario.
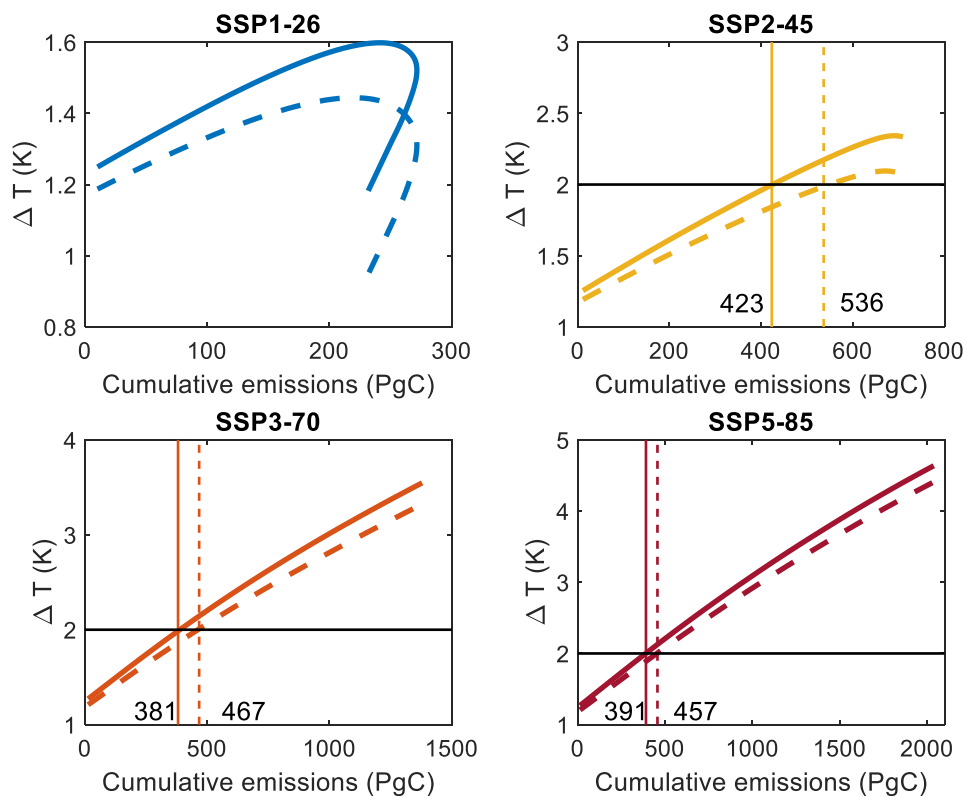
Figure 4. Relationship between global air surface temperature difference to pre-industrial temperature and the cumulative emission of CO_2 from 2024 until 2099 for different emission scenarios and the two model simulations FOK (solid lines) and MMK (dashed lines). Horizontal lines indicate a temperature change threshold of 2K, and vertical lines and numbers indicate the respective cumulative emissions since 2024 to reach that temperature change target.

These differences in the projected land sinks do have clear consequences for the Transient Climate Response to Cumulative Emissions of Carbon Dioxide (TCRE) and hence the remaining anthropogenic carbon budgets under different emission scenarios. Usually, there is a quasi-linear relationship between the cumulative emission and the temperature change (Fig. 4). Under reduced emissions of SSP1-26 scenario, ocean and land C uptake may remain high (blue curves in Fig. 3), leading to a hysteresis in the TCRE (Charles D. Koven, Sanderson, & Swann, 2023). Such hysteresis is not visible in the other scenarios (Fig. 4) because emission reductions are not strong enough

(Fig. 2). Interestingly, the relationship is less steep and more non-linear for the MMK model for all scenarios. From the TCRE the remaining carbon budget for a certain temperature threshold can be estimated (Canadell et al., 2023). In Fig. 4, the vertical lines indicate the amount of emissions since 2024 that - according to this model - can be still emitted in order to keep warming below the threshold of 2 °C warming compared to the pre-industrial situation, which is indicated by the horizontal line. We skip this analysis for scenario SSP1-26 results because the MMK model fails to reach a 2 °C increase at all (Fig. 4). For the other emission scenarios, the FOK model suggests 381 to 423 Pg C that can be emitted to the atmosphere in order to keep warming below 2 °C compared to pre-industrial temperature (Fig. 4). These estimates are slightly higher than the median remaining C budget estimated by CMIP6 experiments using ESMs of 370 Pg C (table 5.8, (Canadell et al., 2023)). Importantly, when assuming a Michaelis-Menten kinetics of respiration (MMK), the remaining C budget is higher and range between 457-536 Pg C. This is due to flatter slopes of these model results (Fig. 4).

Table 2. Terrestrial carbon-climate feedback (Pg C) for different representations of respiration in the model. Shown is the difference of model results accounting for the feedback and excluding it based on the temporal change in atmospheric carbon content between 2080-2100 and 1850-1900.

	First-order kinetics (FOK)	Michaelis-Menten kinetics (MMK)
SSP1-26	379	920
SSP2-45	423	955
SSP3-70	431	959
SSP5-85	498	1019

Using the first-order kinetics approach of respiration (FOK), I estimate a carbon-climate feedback of 379 to 498 Pg C when comparing the average CO_2 concentration of the period 2080-2100 with pre-industrial conditions, depending on the emission scenario (Table 2). This translates into feedback factors of 1.2 to 1.4 (Table 3), which are similar to previous estimates (Lade et al., 2018). Interestingly, the strength of the feedback mechanism as expressed by the feedback factor decreases with increasing carbon emissions (Table 3), i.e. the internal Earth system interactions are more important under reduced anthropogenic emissions. However, when assuming Michaelis-Menten kinetics of respiration, this carbon-climate feedback strength is higher (Table 3) depending on the underlying scenario.

Table 3. Feedback factor of the terrestrial carbon-climate feedback for different representations of respiration in the model. Shown is the difference of model results accounting for the feedback and excluding it based on the temporal change in atmospheric carbon content between 2080-2100 and 1850-1900.

	First-order kinetics (FOK)	Michaelis-Menten kinetics (MMK)
SSP1-26	1.41	2.0
SSP2-45	1.31	1.71
SSP3-70	1.23	1.52

SSP5-85	1.21	1.43	

The FOK model estimates the sensitivity of the land carbon change to increasing atmospheric CO2 concentration (β, Table 4) to be 1.4 Pg C ppm^{-1} assuming the high-emission scenario SSP5-8.5. This is similar to CMIP4 model runs using the high-emission scenario SREAS A2 (Friedlingstein et al., 2006) and at the higher end of the range of CMIP6 model results without considering the N cycle in 4xCO2 experiments (Arora et al., 2020). Interestingly, the sensitivity increases towards scenarios assuming less emissions (Table 4), and the sensitivity is higher when assuming a Michaelis-Menten kinetics of respiration (Table 4). The land carbon change sensitivity to climate change (γ, Table 4) is estimated at -117 Pg C K^{-1} in this case. This is at the higher end of the range for the previously mentioned ESM results (Arora et al., 2020; Friedlingstein et al., 2006). This parameter is also more negative when assuming Michaelis-Menten kinetics or when considering a lower emission scenario (Table 4).

Table 4. Sensitivities of the land carbon change to changing atmospheric carbon dioxide (β, Pg C ppm^{-1}) and temperature (γ, Pg C K^{-1}) for different representations of respiration in the model (FOK and MMK).

	β, Pg C ppm^{-1}, first-order kinetics (FOK)	β, Pg C ppm^{-1}, Michaelis-Menten kinetics (MMK)	γ, Pg C K^{-1}, first-order kinetics (FOK)	γ, Pg C K^{-1}, Michaelis-Menten kinetics (MMK)
SSP1-26	3.4	9.8	-133	-218
SSP2-45	2.3	5.4	-125	-204
SSP3-70	1.6	3.4	-124	-198
SSP5-85	1.4	2.7	-117	-187

4 Discussion

Besides gross primary productivity, ecosystem respiration is one of the main land-atmosphere carbon exchange processes (Friedlingstein et al., 2023). The underlying biochemical processes are complex and mathematical models of simplified net reactions are usually applied in Earth System Models: Either assuming a first-order chemical reaction of carbon and oxygen to carbon dioxide and applying Equation 1, or considering the underlying enzymatic reactions and hence applying Equation 2. The epistemic uncertainty in projecting future land-atmosphere exchange of CO_2, climate and the related biogeochemical feedbacks underlying these assumptions have been addressed in this paper. Model parameters have been chosen based on literature values, and to fit published historical carbon and temperature changes (section 2.3) for the first-order kinetics approach (FOK). For the Michaelis Menten kinetics model (MMK), we selected parameter values such that results are also similar to Global Carbon Budget estimates and the FOK model during the pre-industrial period. Interestingly, effects of anthropogenic carbon emissions on future land sink dynamics differ between both model versions, with several Pg C per year higher uptake by land when assuming Michaelis-Menten kinetics for respiration (Fig. 3). Such higher land carbon uptake leads to a lower ocean carbon sink hence increasing differences between land and ocean sinks. In addition, the projected global surface temperature change until 2100 is lower in the MMK model (Fig. 3), i.e. a lower temperature change response to cumulative carbon emissions (Fig. 4). Since increasing surface temperature

276 will lead to an additional CO_2 release from land to the atmosphere, there is the positive carbon-climate feedback

277 mechanism (Arneth et al., 2010), and here I asked the question, is there also an effect of the respiration model

278 structure on this feedback strength?

279 Indeed, this feedback roughly doubles when assuming Michaelis-Menten kinetics, and it is higher for strong carbon

280 emission scenarios (Table 2). As a consequence, the model results imply a 66 Pg C (SSP5-85) to 113 Pg C (SSP2-

281 45) higher remaining anthropogenic carbon budget to keep warming below 2 °C above pre-industrial levels only

282 because we assume an alternative model structure for respiration. These estimates are similar to estimates of

283 additional warming-induced C loss from permafrost-affected soils until 2100 of 10-100 Pg C (C. D. Koven et al.,

284 2015). Other additional Earth system feedbacks currently not represented in Earth system models (section 5.5.2.2.5

285 in (Canadell et al., 2023)), and additional Geophysical Uncertainties like non- CO_2 forcing or emission uncertainty

286 (Table 5.8 in (Canadell et al., 2023)) are also of the same order of magnitude. Shall we assume a linear or non-

287 linear dependence of respiration on the amount of substrate? This assumption influences the internal land carbon

288 dynamics, because in the latter case respiration does not respond to higher substrate availability in the same way

289 as in the linear model. This is also visible when looking at the sensitivities of the land carbon change to CO_2 change

290 (β, Table 4) which roughly double when assuming Michaelis-Menten kinetics because the response of respiration

291 to higher substrate availability is lower.

292 I applied a simplified model of global biogeochemical feedback mechanisms, considering only one terrestrial

293 carbon pool and no explicit pool of microbial biomass and microbial functions. Therefore, many specific

294 underlying processes and interactions of ecosystem components are neglected. For example, an increase in

295 heterotrophic respiration due to increasing plant productivity and carbon input to soils (priming effect, (Fontaine

296 et al., 2007; Keuper et al., 2020)), or changing microbial community structure as a response to climate change

297 (Glassman et al., 2018) is not considered. Nutrient limitation of vegetation productivity (Hungate, Dukes, Shaw,

298 Luo, & Field, 2003) is only implicitly parametrized in Equations 3 and 4 through a logarithmic response function

299 of GPP to CO_2. Hence, I do not quantify the effects of nutrient availability on the carbon-climate feedback in

300 addition to the effects of either respiration model used. When assuming a MMK model, increasing CO_2 leads to

301 higher increase in land C stocks (β, Table 4) due to lower respiration. However, this mechanism can, for instance,

302 also lock more nutrients in soil organic matter hence change the response function of GPP to CO_2. When

303 considering nutrient processes, land C change sensitivities to CO_2 and temperature have been shown to be much

304 smaller (Arora et al., 2020). In addition, climate change is expressed as a temperature change in this model and

305 precipitation effects on carbon cycle functions (Jung et al., 2017) are not taken into account. Therefore, the

306 presented results are first conservative estimates which should be verified using a state-of-the-art ESM including

307 nutrient cycles and Michaelis-Menten kinetics (Yu et al., 2020). Still, the presented results point to the importance

308 to communicate and address existing structural uncertainties in Earth System Models. Just by assuming an

309 underlying Michaelis-Menten kinetics of respiration processes leads to distinct projections of future respiration

310 and the carbon-climate feedback mechanism. These results also demonstrate the need for novel research clarifying

311 a valid process-based model structure of ecosystem respiration.

312 **5 Conclusions**

313 Two major gross carbon fluxes govern the recent land carbon sink, photosynthesis and respiration. While detailed

314 process-based photosynthesis models have been developed and applied in Earth System Models, how to model

respiration processes remains unclear. The model structure of respiration alone can lead to a doubling of the carbon-climate feedback estimate over the 21st century. Depending on the underlying emission scenario, that translates into a difference of the remaining carbon budget to keep global warming below 2 °C of 66 Pg C (SSP5-85) to 113 Pg C (SSP2-45). These results show the importance of an increased understanding of the mathematical model structure of respiration processes in Earth System Models for more reliably projecting future carbon dynamics and climate, related feedback mechanisms, and hence to estimate a valid remaining anthropogenic carbon budget.

Code availability

MATLAB code of the model versions applied is available via github.

Data availability

All required data to run the model and reproduce the results is available online and open access.

Author contribution CB designed the study, wrote the computer code, downloaded and interpolated the emission data, run the models, analysed the results and wrote the manuscript.

Competing interests CB declares that he has no conflict of interest.

Acknowledgements CB acknowledges financial support by Deutsche Forschungsgemeinschaft through the Heisenberg program (508047523).

References

Alexandrov, G. A., Oikawa, T., & Yamagata, Y. (2003). Climate dependence of the CO2 fertilization effect on terrestrial net primary production. *Tellus Series B-Chemical and Physical Meteorology, 55*(2), 669-675. doi:DOI 10.1034/j.1600-0889.2003.00021.x

Arneth, A., Harrison, S. P., Zaehle, S., Tsigaridis, K., Menon, S., Bartlein, P. J., . . . Vesala, T. (2010). Terrestrial biogeochemical feedbacks in the climate system. *Nature Geoscience, 3*(8), 525-532. doi:10.1038/ngeo905

Arora, V. K., Katavouta, A., Williams, R. G., Jones, C. D., Brovkin, V., Friedlingstein, P., . . . Ziehn, T. (2020). Carbon–concentration and carbon–climate feedbacks in CMIP6 models and their comparison to CMIP5 models. *Biogeosciences, 17*(16), 4173-4222. doi:10.5194/bg-17-4173-2020

Brovkin, V., Boysen, L., Raddatz, T., Gayler, V., Loew, A., & Claussen, M. (2013). Evaluation of vegetation cover and land-surface albedo in MPI-ESM CMIP5 simulations. *Journal of Advances in Modeling Earth Systems, 5*(1), 48-57. doi:https://doi.org/10.1029/2012MS000169

Canadell, J. G., Monteiro, P. M. S., Costa, M. H., Cotrim da Cunha, L., Cox, P. M., Eliseev, A. V., . . . Zickfeld, K. (2023). Global Carbon and Other Biogeochemical Cycles and Feedbacks. In C. Intergovernmental Panel on Climate (Ed.), *Climate Change 2021 – The Physical Science Basis: Working Group I Contribution to the Sixth Assessment Report of the Intergovernmental Panel on Climate Change* (pp. 673-816). Cambridge: Cambridge University Press.

Cox, P. M., Betts, R. A., Jones, C. D., Spall, S. A., & Totterdell, I. J. (2000). Acceleration of global warming due to carbon-cycle feedbacks in a coupled climate model. *Nature, 408*(6809), 184-187.

Cramer, W., Bondeau, A., Woodward, F. I., Prentice, I. C., Betts, R. A., Brovkin, V., . . . Young-Molling, C. (2001). Global response of terrestrial ecosystem structure and function to CO2 and climate change: results from six dynamic global vegetation models. *Global Change Biology, 7*(4), 357-373. Retrieved from http://onlinelibrary.wiley.com/doi/10.1046/j.1365-2486.2001.00383.x/full

Fontaine, S., Barot, S., Barré, P., Bdioui, N., Mary, B., & Rumpel, C. (2007). Stability of organic carbon in deep soil layers controlled by fresh carbon supply. *Nature, 450*(7167), 277-U210. doi:10.1038/nature06275

Friedlingstein, P., Cox, P., Betts, R., Bopp, L., Von Bloh, W., Brovkin, V., . . . Zeng, N. (2006). Climate-carbon cycle feedback analysis: Results from the C⁴MIP model intercomparison. *Journal of Climate, 19*(14), 3337-3353.

Friedlingstein, P., Dufresne, J. L., Cox, P. M., & Rayner, P. (2003). How positive is the feedback between climate change and the carbon cycle? *Tellus B: Chemical and Physical Meteorology, 55*(2), 692-700. doi:10.3402/tellusb.v55i2.16765

Friedlingstein, P., O'Sullivan, M., Jones, M. W., Andrew, R. M., Bakker, D. C. E., Hauck, J., . . . Zheng, B. (2023). Global Carbon Budget 2023. *Earth Syst. Sci. Data, 15*(12), 5301-5369. doi:10.5194/essd-15-5301-2023

Gidden, M. J., Riahi, K., Smith, S. J., Fujimori, S., Luderer, G., Kriegler, E., . . . Takahashi, K. (2019). Global emissions pathways under different socioeconomic scenarios for use in CMIP6: a dataset of harmonized emissions trajectories through the end of the century. *Geosci. Model Dev., 12*(4), 1443-1475. doi:10.5194/gmd-12-1443-2019

Glassman, S. I., Weihe, C., Li, J. H., Albright, M. B. N., Looby, C. I., Martiny, A. C., . . . Martiny, J. B. H. (2018). Decomposition responses to climate depend on microbial community composition. *Proceedings of the National Academy of Sciences of the United States of America, 115*(47), 11994-11999. doi:10.1073/pnas.1811269115

Hansen, J., Lacis, A., Rind, D., Russell, G., Stone, P., Fung, I., . . . Lerner, J. (1984). Climate Sensitivity: Analysis of Feedback Mechanisms. In *Climate Processes and Climate Sensitivity* (pp. 130-163).

Heinze, C., Eyring, V., Friedlingstein, P., Jones, C., Balkanski, Y., Collins, W., . . . Vancoppenolle, M. (2019). ESD Reviews: Climate feedbacks in the Earth system and prospects for their evaluation. *Earth Syst. Dynam., 10*(3), 379-452. doi:10.5194/esd-10-379-2019

Hugelius, G., Strauss, J., Zubrzycki, S., Harden, J. W., Schuur, E. A. G., Ping, C.-L., . . . Kuhry, P. (2014). Estimated stocks of circumpolar permafrost carbon with quantified uncertainty ranges and identified data gaps. *Biogeosciences, 11*(23), 6573-6593. doi:10.5194/bg-11-6573-2014

Hungate, B. A., Dukes, J. S., Shaw, M. R., Luo, Y. Q., & Field, C. B. (2003). Nitrogen and climate change. *Science, 302*(5650), 1512-1513. doi:DOI 10.1126/science.1091390

Jones, C. D., Ziehn, T., Anand, J., Bastos, A., Burke, E., Canadell, J. G., . . . Yun, J. (2023). RECCAP2 Future Component: Consistency and Potential for Regional Assessment to Constrain Global Projections. *Agu Advances, 4*(6), e2023AV001024. doi:https://doi.org/10.1029/2023AV001024

Jones, C. D., Ziehn, T., Anand, J., Bastos, A., Burke, E., Canadell, J. G., . . . Yun, J. M. (2023). RECCAP2 Future Component: Consistency and Potential for Regional Assessment to Constrain Global Projections. *Agu Advances, 4*(6). doi:ARTN e2023AV001024

10.1029/2023AV001024

Jung, M., Reichstein, M., Schwalm, C. R., Huntingford, C., Sitch, S., Ahlström, A., . . . Zeng, N. (2017). Compensatory water effects link yearly global land CO

sink changes to temperature. *Nature, 541*(7638), 516-520. doi:10.1038/nature20780

Keuper, F., Wild, B., Kummu, M., Beer, C., Blume-Werry, G., Fontaine, S., . . . Dorrepaal, E. (2020). Carbon loss from northern circumpolar permafrost soils amplified by rhizosphere priming. *Nature Geoscience, 13*(8), 560-565. doi:10.1038/s41561-020-0607-0

Koven, C. D., Sanderson, B. M., & Swann, A. L. S. (2023). Much of zero emissions commitment occurs before reaching net zero emissions. *Environmental Research Letters, 18*(1), 014017. doi:10.1088/1748-9326/acab1a

Koven, C. D., Schuur, E. A. G., Schädel, C., Bohn, T. J., Burke, E. J., Chen, G., . . . Turetsky, M. (2015). A simplified, data-constrained approach to estimate the permafrost carbon–climate feedback. *Philosophical Transactions of the Royal Society A: Mathematical, Physical and Engineering Sciences, 373*(2054), 20140423. doi:10.1098/rsta.2014.0423

Lade, S. J., Donges, J. F., Fetzer, I., Anderies, J. M., Beer, C., Cornell, S. E., . . . Steffen, W. (2018). Analytically tractable climate--carbon cycle feedbacks under 21st century anthropogenic forcing. *Earth System Dynamics, 9*(2), 507-523. Retrieved from https://www.earth-syst-dynam.net/9/507/2018

Lloyd, J., & Taylor, J. A. (1994). On the temperature dependence of soil respiration. *Functional Ecology, 8*, 315-323.

Nijsse, F. J. M. M., Cox, P. M., & Williamson, M. S. (2020). Emergent constraints on transient climate response (TCR) and equilibrium climate sensitivity (ECS) from historical warming in CMIP5 and CMIP6 models. *Earth System Dynamics, 11*(3), 737-750. doi:10.5194/esd-11-737-2020

O'Sullivan, M., Friedlingstein, P., Sitch, S., Anthoni, P., Arneth, A., Arora, V. K., . . . Zaehle, S. (2022). Process-oriented analysis of dominant sources of uncertainty in the land carbon sink. *NATURE COMMUNICATIONS, 13*(1). doi:ARTN 4781

10.1038/s41467-022-32416-8

421   Reichstein, M., & Beer, C. (2008). Soil respiration across scales: the importance of a model-‐data integration
422   framework for data interpretation. *Journal of Plant Nutrition and Soil Science, 171*(3), 344-354.
423   Retrieved from http://onlinelibrary.wiley.com/doi/10.1002/jpln.200700075/full
424   Riahi, K., van Vuuren, D. P., Kriegler, E., Edmonds, J., O'Neill, B. C., Fujimori, S., . . . Tavoni, M. (2017). The
425   Shared Socioeconomic Pathways and their energy, land use, and greenhouse gas emissions implications:
426   An overview. *Global Environmental Change, 42*, 153-168.
427   Sitch, S., Smith, B., Prentice, I. C., Arneth, A., Bondeau, A., Cramer, W., . . . others. (2003). Evaluation of
428   ecosystem dynamics, plant geography and terrestrial carbon cycling in the LPJ dynamic global vegetation
429   model. *Global Change Biology, 9*(2), 161-185. Retrieved from
430   http://onlinelibrary.wiley.com/doi/10.1046/j.1365-2486.2003.00569.x/full
431   Tang, J., Riley, W. J., & Zhu, Q. (2022). Supporting hierarchical soil biogeochemical modeling: version 2 of the
432   Biogeochemical Transport and Reaction model (BeTR-v2). *Geosci. Model Dev., 15*(4), 1619-1632.
433   doi:10.5194/gmd-15-1619-2022
434   Vaughn, L. J. S., & Torn, M. S. (2019). C evidence that millennial and fast-cycling soil carbon are equally sensitive
435   to warming. *Nature Climate Change, 9*(6), 467-+. doi:10.1038/s41558-019-0468-y
436   Wieder, W. R., Bonan, G. B., & Allison, S. D. (2013). Global soil carbon projections are improved by modelling
437   microbial processes. *Nature Climate Change, 3*(10), 909-912. doi:10.1038/nclimate1951
438   Yu, L., Ahrens, B., Wutzler, T., Schrumpf, M., & Zaehle, S. (2020). Jena Soil Model (JSM v1.0; revision 1934):
439   a microbial soil organic carbon model integrated with nitrogen and phosphorus processes. *Geoscientific*
440   *Model Development, 13*(2), 783-803. doi:10.5194/gmd-13-783-2020
441   Zickfeld, K., Eby, M., Matthews, H. D., Schmittner, A., & Weaver, A. J. (2011). Nonlinearity of Carbon Cycle
442   Feedbacks. *Journal of Climate, 24*(16), 4255-4275. doi:https://doi.org/10.1175/2011JCLI3898.1

443

444

445

446